

Burnup Sensitivity Calculation in a Fast Breeder Reactor
with a Generalized Perturbation Theory

Toshikazu Takeda and Takuya Umano

Department of Nuclear Engineering, Faculty of
Engineering, Osaka University*

ABSTRACT

The Williams formula for sensitivity coefficients for burnup properties is extended to take account of the neutronic properties at the end of burnup cycle and to treat the bilinearly weighted neutronic property. The sensitivity coefficients for the burnup properties of a fast breeder reactor are calculated, and the physical meanings of the coefficients are considered. The accuracy of the obtained sensitivity coefficients is verified by comparing the results with those from the direct subtraction calculations.

* 2-1 Yamadaoka, Suita, 565 Osaka, Japan

I. INTRODUCTION

The accurate prediction of neutronic properties during fuel burnup is very important for core designs. The calculated neutronic properties have some uncertainty incurred by errors in the utilized cross sections and the calculational methods. In order to estimate the uncertainty in a large liquid metal fast breeder reactor, P. Hammer proposed a burnup benchmark to Nuclear Energy Agency, committee on reactor physics (NEACRP)¹). Numerical results of neutron multiplication factor, burnup reactivity loss, nuclide number densities and reaction rate ratios at the end of one year burnup were presented from many organizations, and the differences of the results were investigated; the burnup reactivity loss was 1.5 %dk/k in its mean value and the standard variation was about 0.5 %dk/k. Such large uncertainty is due to the differences of the cross section sets used in the analyses.

To investigate such differences, the sensitivity coefficients of neutronic properties during burnup due to cross section changes of individual nuclides are very useful. The sensitivity coefficients can be directly calculated from the difference of two neutronics properties calculated with the original and the perturbed cross section sets; this procedure will be simple if the number of cross section changes is limited. In contrast, when we consider the change of each of multigroup cross sections of many nuclides, the generalized perturbation theory will be powerful because the sensitivities can be easily calculated without performing direct flux calculations with the perturbed cross sections; only a generalized flux needs to be calculated for a relevant neutronic property.

The generalized perturbation theory has been applied first to the calculation of sensitivities of nuclide number densities to

cross section changes in a zero-dimensional steady state problem by Gandini²⁾, and many efforts have been devoted to extend the method to multi-dimensional problems³⁾. However, these studies did not consider the nonlinear interaction between the neutron and nuclide fields: In the sensitivity calculation of nuclide number densities the neutron flux was assumed to be constant over a burnup period.

Williams has derived the practical formula for burnup sensitivity coefficients⁴⁾ by coupling the neutron and nuclide fields:

He divided the burnup period into several time intervals and used the quasi-static approximation for the flux over each time interval. The flux was calculated at the beginning of each time interval by using the nuclide number densities obtained from the burnup equation in the previous time interval.

In burnup analysis of a large fast breeder reactor with a multi-dimensional core model, a flux calculation requires a large amount of computer time. To reduce flux calculations a burnup period (usually one year) is divided into few intervals, and in some cases the period is only one interval, particularly for survey calculations. In such a case the Williams formula needs to be extended to include the flux information at the end of a cycle.

Since his formula uses the flux at the beginning of each interval, the flux at the end of a cycle can not be considered in such a case. Williams derived the burnup sensitivity theory for neutronic properties defined by cross sections, atomic densities and neutron fluxes. But in order to derive a formula for the sensitivity coefficients of bilinearly weighted neutronic properties such as the changes of control rod worths, sodium void worths due to a burnup, it is necessary to include the adjoint

flux -this is not considered in the Williams theory - in the formulation of burnup sensitivity coefficients.

The purpose of this paper is to extend the Williams formula such that the neutronic properties at the end of burnup period can be considered and the bilinear neutronic properties can be treated, and also to show numerical results for burnup sensitivity coefficients in a large fast breeder reactor. We derive sensitivity coefficients using two methods on the basis of a generalized perturbation theory, a variational method and a differential method. The variational method is the same as that adopted by Williams in deriving sensitivity coefficients of linearly weighted neutronic properties. We compare the resultant formulae derived by the two methods.

Burnup sensitivity coefficients are calculated for a demonstration fast breeder reactor. The calculated coefficients are compared with those evaluated from the direct burnup calculations, and we check the applicability of the derived formulae.

II. SENSITIVITY THEORY

We derive the formula for the sensitivity coefficients on the basis of a generalized perturbation theory. For making numerical calculations easy, we followed the Williams procedure. The system considered was divided into several regions, and the average atomic density of nuclide l at time t is denoted by $N_r^l(t)$ in region r . When using the following atomic density vector,

$$\mathbb{N}_r(t) = [N_r^1(t), N_r^2(t), \dots, N_r^m(t)] \quad (1)$$

the nuclide transmutation equation reduces to

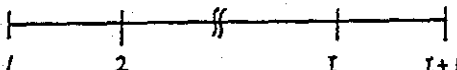
$$\frac{\partial}{\partial t} \mathbb{N}_r(t) = \mathbb{M} \mathbb{N}_r(t) \quad (2)$$

where M is a transmutation matrix, and it is decomposed into the cross section matrix and the decay matrix as follows:

$$M = \langle R \phi \rangle_E + D \quad (3)$$

where R is the neutron reaction matrix whose non-diagonal element R_{ij} is the sum of the microscopic cross section and the yield data for production of nuclide i by nuclide j, and diagonal element R_{ii} is the opposite value of the absorption cross section for nuclide i; D is the decay matrix whose non-diagonal element D_{ij} is the decay constant for nuclide j to i, and diagonal element D_{ii} is the opposite value of the total decay constant for nuclide i.

To calculate the atomic density of each nuclide through burnup we have to calculate the neutron flux. We follow the commonly used procedure for calculating the neutron flux: We divide the exposure period into individual time interval, and at the beginning of each time interval indexed by subscript i we calculate a neutron flux on the basis of a diffusion theory:

$$B_i \phi_i = 0 \quad (i=1, 2, \dots, I+1) \quad (4)$$


where B_i is the diffusion operator. The diffusion parameters which constitute the operator B are evaluated from the number densities calculated by the previous time interval. In the similar way, the adjoint flux is calculated from the adjoint equation:

$$B_i^* \phi_i^* = 0 \quad (i=1, 2, \dots, I+1) \quad (5)$$

where B_i^* is the adjoint operator to B . It is noted that the flux calculation and the adjoint flux calculation are performed at the end of the burnup period to obtain the neutronic properties at that time.

The neutron flux is normalized by using the reactor power at each time interval:

$$P_i = \langle \kappa \sigma_f N \phi_i \rangle_{E,V} \quad (6)$$

where $\langle \rangle_{E,V}$ shows the summation over all energy groups, and the integration over core volume, κ is the energy release per fission, σ_f is the cross section vector composed of microscopic fission cross sections of individual nuclides.

$$\sigma_f = [\sigma_f^1, \sigma_f^2, \dots, \sigma_f^n] = \sigma_f(E, r) \quad (7)$$

In the following we consider the neutronic property which is a function of neutron cross sections σ , atomic densities N , the neutron flux ϕ , and the adjoint neutron flux ϕ^* . The sensitivity coefficient of R due to the cross section change is defined by

$$S = \frac{dR}{R} / \frac{d\sigma}{\sigma} \quad (8)$$

Since the cross section change causes the alternations of the number density dN , the flux $d\phi$, and the adjoint flux $d\phi^*$, the sensitivity coefficient can be expressed by

$$S = \frac{\sigma}{R} \left(\frac{\partial R}{\partial \sigma} + \frac{\partial R}{\partial N} \frac{dN}{d\sigma} + \frac{\partial R}{\partial \phi} \frac{d\phi}{d\sigma} + \frac{\partial R}{\partial \phi^*} \frac{d\phi^*}{d\sigma} \right) \quad (9)$$

The above expression requires calculations of $dN/d\sigma$, $d\phi/d\sigma$ and $d\phi^*/d\sigma$ from burnup calculations with perturbed cross section sets. Accordingly, the computing time becomes enormous when there are many cross section changes. Thus we use a generalized perturbation theory which enables us to efficiently calculate the sensitivity coefficients. We derive a formula for the sensitivity coefficient using two methods, a variational method and a differential method.

2.1 Variational Approach

Williams derived the practical formula for the sensitivity coefficients using a variational method. We extend his formula to treat the neutronic properties at the end of the burnup period and bilinearly weighted neutronic properties. Following his procedure we consider the following functional:

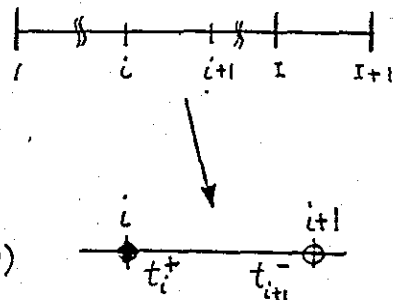
$$K[N, \phi, \phi^*, \sigma]$$

$$= \sum_{i=1}^I \left\langle \int_{t_i^+}^{t_{i+1}^-} dt R \right\rangle_{E,V} + \sum_{i=1}^I \left\langle \int_{t_i^+}^{t_{i+1}^-} dt N^* M N \right\rangle_V$$

$$+ \sum_{i=1}^{I+1} \langle P_i^* B_i \phi_i \rangle_{E,V}$$

$$+ \sum_{i=1}^{I+1} \langle P_i^* B_i^* \phi_i^* \rangle_{E,V}$$

$$+ \sum_{i=1}^{I+1} P_i^* \left\{ P_i - \langle \kappa \phi_f N \phi_i \rangle_{E,V} \right\} \quad (10)$$



where N^* , Γ_i , Γ_i^* and P_i^* are Lagrange multipliers. Unlike the Williams expression for K , the third term, the fourth term and the last term include the summation not only over the beginning of each time interval but also over the end of the burnup period ($i = I + 1$). In addition, the fourth term is included to treat bilinearly weighted neutronic properties. If N and ϕ are exact solutions to the burnup equation, then K reduces to R . An alternation in cross section data will result in

$$K \rightarrow K' = K + \sum_x \left\langle \frac{\partial K}{\partial \sigma_x} \delta \sigma_x \right\rangle_{E,V} + \sum_j \int dt \left\langle \frac{\partial K}{\partial N_j} \delta N_j \right\rangle_{E,V} + \sum_i \left\langle \frac{\partial K}{\partial \phi_i} \delta \phi_i \right\rangle_{E,V} + \sum_i \left\langle \frac{\partial K}{\partial \phi_i^*} \delta \phi_i^* \right\rangle_{E,V}$$

If we can set,

(11)

$$\frac{\partial K}{\partial N_j} = 0, \quad \frac{\partial K}{\partial \phi_i} = 0, \quad \frac{\partial K}{\partial \phi_i^*} = 0 \quad (12)$$

the sensitivity coefficient reduces to

$$S(\sigma_x^g) = \frac{\sigma_x^g}{R} \left[\sum_{i=1}^I \left\langle \int_{t_i^+}^{t_{i+1}^-} dt \frac{\partial R}{\partial \sigma_x^g} \right\rangle_V + \sum_{i=1}^I \left\langle \int_{t_i^+}^{t_{i+1}^-} dt N^* \frac{\partial M}{\partial \sigma_x^g} N \right\rangle_V \right. \\ \left. + \sum_{i=1}^{I+1} \left\langle \Gamma_i^* \frac{\partial B_i}{\partial \sigma_x^g} \phi_i \right\rangle_V + \sum_{i=1}^{I+1} \left\langle \Gamma_i \frac{\partial B_i^*}{\partial \sigma_x^g} \phi_i^* \right\rangle_V \right. \\ \left. - \sum_{i=1}^{I+1} P_i^* \left\langle K \frac{\partial \sigma_x^g}{\partial \sigma_x^g} N \phi_i \right\rangle_V \right] \quad (13)$$

The conditions (12) lead to the following equations for N^* ,

Γ_i, Γ_i^* and P_i^* ; $i = 1, 2, \dots, I$

$$\bullet P_{I+1}^* = \langle \phi_{I+1} \frac{\partial \mathcal{R}}{\partial \phi_{I+1}} \rangle_{E,V} / P_{I+1} \quad (14)$$

$$\bullet P_i^* = \left\{ \langle \int_{t_i^+}^{t_{i+1}^-} dt N^* \langle R \phi \rangle_E N \rangle_V + \langle \int_{t_i^+}^{t_{i+1}^-} dt \phi_i \frac{\partial \mathcal{R}}{\partial \phi_i} \rangle_{E,V} \right\} / P_i \quad (15)$$

$$\bullet B_{I+1} \Gamma_{I+1} = - \frac{\partial \mathcal{R}}{\partial \phi_{I+1}^*} \quad (16)$$

$$\bullet B_i \Gamma_i = - \int_{t_i^+}^{t_{i+1}^-} dt \frac{\partial \mathcal{R}}{\partial \phi_i^*} \quad (17)$$

$$\bullet B_{I+1}^* \Gamma_{I+1}^* = P_{I+1}^* \kappa \sigma_f N_{I+1} - \frac{\partial \mathcal{R}}{\partial \phi_{I+1}} \quad (18)$$

$$\bullet B_i \Gamma_i^* = - \int_{t_i^+}^{t_{i+1}^-} dt \left\{ \frac{\partial \mathcal{R}}{\partial \phi_i} + N^* \frac{\partial M}{\partial \phi_i} N \right\} + P_i^* \kappa \sigma_f N_i \quad (19)$$

$$\bullet N^*(t_{I+1}^-) = \langle \Gamma_{I+1}^* \left(\frac{\partial B_{I+1}}{\partial N_{I+1}} \right) \phi_{I+1} + \Gamma_{I+1} \left(\frac{\partial B_{I+1}^*}{\partial N_{I+1}} \right) \phi_{I+1}^* + \frac{\partial \mathcal{R}}{\partial N_{I+1}} - P_{I+1}^* \kappa \sigma_f \phi_{I+1} \rangle_E \quad (20)$$

$$\bullet - \frac{\partial}{\partial t} N^* = M^t N^* + \left(\frac{\partial \mathcal{R}}{\partial N} \right)_E \quad t: \text{transpose} \quad (21)$$

$$\bullet N_{t_i^-}^* = N_{t_i^+}^* + \langle \Gamma_i^* \frac{\partial B_i}{\partial N_i} \phi_i \rangle_E + \langle \Gamma_i \frac{\partial B_i^*}{\partial N_i} \phi_i^* \rangle_E - \langle P_i^* \kappa \sigma_f \phi_i \rangle_E \quad (22)$$

As it is shown above, N^* shows the discontinuity at each time interval. This jump condition for N^* is expressed by Eq. (22).

The solution algorithm for N^* , P^* , F^* and F is shown in Fig. 1. At the end of a burnup period $F_{t_i}^*$, F_{t_i} , and $P_{t_i}^*$ are calculated from Eqs. (14), (16), and (18). Using the results the initial value of $N_{t_i}^*$ is determined from Eq. (20). N^* is solved from Eq. (21) for the last time interval. Then, F , F^* and P^* are calculated at $t=t_i$. With the value for P^* , F^* and F at $t=t_i$ the value for N^* at t_i^- is computed from Eq. (22). Using this N^* as the final condition we solve N^* for the next time interval. This procedure is followed backwards until $t=0$.

2.2 Differential Approach

We derive the formula for the burnup sensitivity coefficients with a differential approach.

From the equations for the atomic density, the neutron flux, the adjoint flux, the power, we obtain

$$\frac{\partial}{\partial t} N = \lambda N$$

$$\frac{d}{dt} \left(\frac{\partial N}{\partial \sigma} \right) = \left(\frac{\partial \lambda}{\partial \sigma} + \frac{\partial \lambda}{\partial N_i} \frac{dN_i}{d\sigma} \right) N + \lambda \frac{dN}{d\sigma} \quad (23)$$

$$B_i \phi_i = 0$$

$$\left(\frac{\partial B_i}{\partial \sigma} + \frac{\partial B_i}{\partial N_i} \frac{dN_i}{d\sigma} \right) \phi_i + B_i \frac{d\phi_i}{d\sigma} = 0 \quad (24)$$

$$B_i^* \phi_i^* = 0$$

$$\left(\frac{\partial B_i^*}{\partial \sigma} + \frac{\partial B_i^*}{\partial N_i} \frac{dN_i}{d\sigma} \right) \phi_i^* + B_i^* \frac{d\phi_i^*}{d\sigma} = 0 \quad (25)$$

$$P_i = \langle \kappa \sigma_f N \phi_i \rangle_{E,V}$$

$$\frac{\partial P_i}{\partial \sigma} + \kappa \sigma_f N_i \frac{d\phi_i}{d\sigma} + \phi_i \kappa \sigma_f \frac{dN_i}{d\sigma} = 0 \quad (26)$$

Multiplying the above Eqs. by N^* , Γ^* , Γ and P^* , and adding the resultant Eqs. leads to

$$\begin{aligned}
 & \sum_{i=1}^I \int_{t_i^+}^{t_{i+1}^-} dt \left\langle \frac{dN}{d\sigma} \left\{ -\frac{\partial N^*}{\partial t} - M^* N^* \right\} \right\rangle_{E,V} \\
 & + \sum_{i=1}^I \left\langle \frac{d\phi_i}{d\sigma} \left\{ -B_i^* \Gamma_i^* - \int_{t_i^+}^{t_{i+1}^-} dt N^* \frac{\partial M}{\partial \phi_i} N + P_i^* \kappa \sigma_f N_i \right\} \right\rangle_{E,V} \\
 & + \sum_{i=1}^I \left\langle \frac{d\phi_i^*}{d\sigma} \left\{ -B_i \Gamma_i \right\} \right\rangle_{E,V} \\
 & + \left\langle \frac{d\phi_{I+1}}{d\sigma} \left\{ -B_{I+1}^* \Gamma_{I+1}^* + P_{I+1}^* \kappa \sigma_f N_{I+1} \right\} \right\rangle_{E,V} + \left\langle \frac{d\phi_{I+1}^*}{d\sigma} \left\{ -B_{I+1} \Gamma_{I+1} \right\} \right\rangle_{E,V} \\
 & + \left\langle \frac{dN_{I+1}}{d\sigma} \left\{ P_{I+1}^* \kappa \sigma_f \phi_{I+1} - \Gamma_{I+1}^* \frac{\partial B_{I+1}}{\partial N_{I+1}} \phi_{I+1} - \Gamma_{I+1} \frac{\partial B_{I+1}^*}{\partial N_{I+1}} \phi_{I+1}^* + N_{I+1}^* \right\} \right\rangle_{E,V} \\
 & + \sum_{i=1}^I \left\langle \frac{dN_i}{d\sigma} \left\{ P_i^* \kappa \sigma_f \phi_i - \Gamma_i^* \frac{\partial B_i}{\partial N_i} \phi_i - \Gamma_i \frac{\partial B_i^*}{\partial N_i} \phi_i^* - N_{i+}^* + N_{i-}^* \right\} \right\rangle_{E,V} \\
 & = \sum_{i=1}^I \int_{t_i^+}^{t_{i+1}^-} dt \left\langle N \frac{\partial M}{\partial \sigma} N \right\rangle_{E,V} + \sum_{i=1}^{I+1} \left\langle \Gamma_i^* \frac{\partial B_i}{\partial \sigma} \phi_i \right\rangle_{E,V} \\
 & + \sum_{i=1}^{I+1} \left\langle \Gamma_i \frac{\partial B_i}{\partial \sigma} \phi_i^* \right\rangle_{E,V} - \sum_{i=1}^{I+1} \left\langle P_i^* \frac{\partial P}{\partial \sigma} \right\rangle_{E,V} \quad (27)
 \end{aligned}$$

Comparing Eq. (27) with the following expression for the sensitivity coefficient:

$$\begin{aligned}
\frac{dR}{d\sigma} = & \frac{\partial R}{\partial \sigma} + \sum_{i=1}^I \int_{t_i^+}^{t_{i+1}^-} \left\langle \frac{dN}{d\sigma} \frac{\partial R}{\partial N} \right\rangle_{E,V} + \sum_{i=1}^I \left\langle \frac{d\phi_i}{d\sigma} \int_{t_i^+}^{t_{i+1}^-} dt \frac{\partial R}{\partial \phi_i} \right\rangle_{E,V} \\
& + \sum_{i=1}^{I+1} \left\langle \frac{d\phi_i^*}{d\sigma} \int_{t_i^+}^{t_{i+1}^-} dt \frac{\partial R}{\partial \phi_i^*} \right\rangle_{E,V} + \left\langle \frac{dN_{I+1}}{d\sigma} \frac{\partial R}{\partial N_{I+1}} \right\rangle_{E,V} \\
& + \left\langle \frac{d\phi_{I+1}}{d\sigma} \frac{\partial R}{\partial \phi_{I+1}} \right\rangle_{E,V} + \left\langle \frac{d\phi_{I+1}^*}{d\sigma} \frac{\partial R}{\partial \phi_{I+1}^*} \right\rangle_{E,V} \quad (28)
\end{aligned}$$

we can see that, if we determine N^* , Γ^* , Γ and P^* to satisfy Eqs. (14)~(22), Eq. (28) yields the same sensitivity coefficient as Eq. (13). Thus the both variational and differential approaches lead to the same formula for the burnup sensitivity coefficient.

III. BURNUP SENSITIVITIES IN A FAST REACTOR

As an application of the derived formulation, we calculate sensitivity coefficients of burnup neutronic properties of a demonstration fast breeder reactor. The main characteristics of the core are listed in Table 1. Figure 2 show the RZ model used in calculations; control rods are withdrawn and control rod positions are represented by three ring regions. Figure 3 shows the burnup chain of calculated nuclides. In the calculational model, while decay of ^{241}Pu to ^{241}Am is considered, ^{241}Am itself is neglected. The reactor thermal power is 2480MW, burnup period is 292 days. This period comes from 365 days multiplied by 80 percent of the operation ratio. The time step is only one, so we calculated the flux and the adjoint flux at the beginning of the period and at the end. Also we used a constant flux approx-

imation over the period ; the flux and the adjoint flux change only at the end of fuel cycle. We calculated the sensitivity coefficients of k_{eff} 's at the beginning and the end of a equilibrium fuel cycle, the burnup reactivity loss, atomic densities at the end of a cycle and the breeding ratio. Calculations were performed in four energy groups with a cross section set obtained from the JENDL-2 library. The upper energy boundaries of the four groups are 10.5 MeV, 1.5 MeV, 0.5 MeV, 0.2 MeV and 0.1 MeV, respectively.

1) Number density

Table 2 shows the sensitivity coefficients of heavy atomic number densities to various cross sections at EOC. The number densities at BOC are fixed, and the sensitivity is zero at that time. From the table it is apparent that the sensitivities have strong spatial dependence. For example, the sensitivity of the ^{239}Pu number density to $^{239}\text{Pu}(n,\gamma)$ cross section is negative in the inner core, in the outer core, in the axial blanket, and in the radial blanket region adjacent to the core, but it is positive in the radial blanket far from the core. In the core the increase of $^{239}\text{Pu}(n,\gamma)$ cross section leads to larger decrease of ^{239}Pu through neutron absorption. In addition the increase leads to harder neutron spectrum in the core. Thus the neutron fluxes in the radial and axial blanket regions increase due to the incoming of high energy neutrons from the core. In the axial blanket and the radial blanket near the core, ^{239}Pu number densities are rather large. Thus the increase of the flux and the absorption cross section of ^{239}Pu lead to decrease of ^{239}Pu

number densities in these regions. However, in the radial blanket region apart from the core, the buildup of ^{239}Pu is mainly due to the conversion from ^{238}U because of the small number density of ^{239}Pu . Thus the increase of the flux in that region leads to the increase of the ^{239}Pu number density.

For ^{241}Pu number density, the sensitivities to $^{239}\text{Pu}(n,f)$ cross section are positive in the core, and negative in the blanket. This is due to the following fact: In the core, the increase of $^{239}\text{Pu}(n,f)$ cross section decreases the flux because of constant power, and the consumption of ^{241}Pu due to fission decreases. However, in the blanket, the buildup of ^{241}Pu from the $^{240}\text{Pu}(n,\gamma)$ reaction decrease by the flux decrease.

Table 3 shows the component-wise sensitivities of ^{239}Pu number densities in the inner core. For the sensitivities to the capture cross sections of ^{238}U and ^{239}Pu , the number density term contributes mainly. However, the flux and the power terms also make remarkable contributions to the sensitivities for the fission cross sections of the two nuclides. For the sensitivities of ^{240}Pu , ^{241}Pu , ^{242}Pu , ^{235}U , FP and structural materials the number density term is zero because of no transmutation to ^{239}Pu through the burnup chain. For the FP capture cross section only the flux term remains.

2) k_{eff}

Table 4 shows the total (integrated over energy groups) sensitivity coefficients of k_{eff} and their components to various cross sections. Sensitivities to the cross sections of structural materials show a little difference between BOC and EOC. On

the contrary, for the sensitivities to $^{238}\text{U}(n,r)$, $^{239}\text{Pu}(n,f)$, $^{239}\text{Pu}(n,r)$, $^{240}\text{Pu}(n,r)$, $^{241}\text{Pu}(n,f)$, $^{241}\text{Pu}(n,r)$ and $\text{FP}(n,r)$ cross sections differences are more than 10%. In section is larger than that at BOC by about 40%.

Let's consider the component wise sensitivities of k_{eff} at EOC.

The direct term agrees well with the sensitivity at BOC. This is due to the fact that the direct term means the sensitivity in the case where the cross section is altered only at EOC; the sensitivity at BOC is also for the case where the cross section is altered at the immediate time point. The sensitivities in table 4 are for the case where the cross section is altered from BOC to EOC, thus the number density and flux are changed during the burnup period. Let's consider the sensitivity to $^{238}\text{U}(n,r)$ cross section. The increase of the $^{238}\text{U}(n,r)$ cross section leads to the production of ^{239}Pu ; 1% increase of the $^{238}\text{U}(n,r)$ cross section leads to 0.2% increase of ^{239}Pu at EOC as is seen from Table 2; sensitivities of k_{eff} at BOC (sensitivities without the number density effect and the flux effect) to the $^{239}\text{Pu}(n,f)$ and (n,r) cross sections are -0.444 and -0.055, respectively as shown in Table 4; then the 1% increase of the $^{238}\text{U}(n,r)$ cross section leads to 0.08% increase in k_{eff} at EOC. This increase mainly corresponds to the number density term in table 3. Next let's consider the sensitivities to fission and capture cross sections of Pu-239. The sensitivity to the capture cross section increase in its absolute value due to burnup, though that to the fission cross section decreases. We explain

this difference. The increase of either the fission or the capture cross section leads to the decrease of ^{239}Pu number density at EOC, and therefore the both values of the number density terms are negative. However, the direct terms is positive for the fission cross section and negative for the capture cross section. Thus, the sensitivity changes due to burnup show the inverse trend for the two cross sections. Next we consider the sensitivity to fission product capture cross section. It is seen that the direct term at EOC is about twice as large as that at BOC because of the buildup of fission product at EOC ; the number density term is opposite in its sign to the direct term ; Thus the sensitivity at EOC is about 40% larger than that at BOC. Furthermore it is generally observed that the indirect terms make a remarkable contribution for the capture cross sections of ^{238}U , ^{239}Pu , ^{240}Pu , ^{241}Pu and ^{242}Pu . For fission cross sections the contribution of the indirect terms is less than 20%, and for the transport and scattering cross sections the contribution is much smaller, at most 5%. The power term has a contribution only for fission cross sections.

To see the energy dependence of the change of the sensitivity coefficient we compare in Table 5 four group sensitivities of k_{eff} at BOC and EOC to the $^{238}\text{U}(n,\gamma)$, $^{239}\text{Pu}(n,\gamma)$, $^{239}\text{Pu}(n,f)$, $^{241}\text{Pu}(n,\gamma)$, $^{241}\text{Pu}(n,f)$, and $\text{FP}(n,\gamma)$ cross sections. Relative changes of the sensitivities between BOC and EOC to the capture cross sections are larger in lower energy groups; those to the fission cross sections are almost constant in groups. This is due to different contributions of the flux term. Different

neutron spectra are produced according to the cross section change in each group. For example, the increase of the fourth group capture cross section of ^{238}U yields a harder spectrum than that for the first group.

3) Burnup reactivity loss

Table 6 shows the total sensitivity coefficient of burnup reactivity loss. The $^{238}\text{U}(n,\gamma)$, $^{238}\text{U}(n,f)$, $^{239}\text{Pu}(n,\gamma)$, $^{239}\text{Pu}(n,f)$, $^{240}\text{Pu}(n,\gamma)$, $^{241}\text{Pu}(n,\gamma)$, $^{241}\text{Pu}(n,f)$ and $\text{FP}(n,\gamma)$ cross sections have high sensitivities. Among them the sensitivity to $^{238}\text{U}(n,\gamma)$ cross section is the largest. Table 7 shows the energy dependent sensitivities to the $^{238}\text{U}(n,\gamma)$ and $^{239}\text{Pu}(n,f)$ cross sections. It is seen that the number density term makes a main contribution for the $^{238}\text{U}(n,\gamma)$ cross section, but the direct and power terms have remarkable contributions for $^{239}\text{U}(n,f)$ cross section.

IV VERIFICATION OF SENSITIVITY COEFFICIENT

As a verification test we calculated sensitivity coefficients by direct subtractions of neutronic properties calculated with original and perturbed cross sections, and compared the results with those obtained from the generalized depletion perturbation theory. The cross sections for $^{238}\text{U}(n,\gamma)$, $^{239}\text{Pu}(n,f)$ and $\text{FP}(n,\gamma)$ reactions are separately changed by 10 % in all groups. Table 8 compared the sensitivity coefficients of k_{eff} at BOC and EOC, burnup reactivity loss and ^{239}Pu number densities at the inner core region (1) and at the radial blanket region (1)

at EOC. In general, good agreement is seen for the sensitivity coefficients obtained from the two methods, though the difference is large for the sensitivity coefficients of burnup reactivity loss and ^{239}Pu number density at blanket due to $\text{FP}(n,\gamma)$ cross section.

V CONCLUSIONS

We have extended the Williams formula for the burnup sensitivity coefficient, which is based on the variational method, to take into account the neutronic properties at EOC and to consider the bilinearly weighted neutronic properties. The extended formula was the same as that derived from the differential approach. The sensitivity coefficients for the burnup properties of a fast breeder reactor were calculated, and the physical meanings of the coefficients were considered. The accuracy of the obtained sensitivity coefficients was verified by comparing the results with those from the direct subtraction calculations.

ACKNOWLEDGMENT

The authors would like to express their deep appreciation to Dr. S. Iijima, Dr. T. Kamei and Dr. T. Yoshida for their useful discussion in developing the formula and in numerical calculations.

REFERENCES

- 1) G.Palmiotti and M.Salvatores, NEACRP-A-504 (12th August 1982)
Proceeding of the NEACRP Specialists' Meeting "NEACRP LMFBR
Benchmark Calculation Intercomparison for Fuel Burn-up".
- 2) A.Gandini, "Time-Dependent Generalized Perturbation Theory
for burn-up Analysis", CHEN RT/FI(75) 4, Comitato Nazionale
per l'Energia Nucleare , Rome (1975).
- 3) A.Gandini, M.Salvatores, and L.Tondinelli, Nucl. Sci.Eng.,
62,339 (1977).
- 4) M.L.Williams, Nucl.Sci.Eng., 70,20 (1979).

Table 1. Main characteristics of a large fast breeder reactor used for burnup calculation

Characteristics	
Reactor power	2480 MWth
Burnup period	292 days
Core height	100 cm
Equivalent Core diameter	320 cm
Core volume (with CRP)	8040 litter
Axial Blanket thickness	35 cm
Radial Blanket thickness	25 cm
Pu isotopic ratio	$^{239}\text{Pu} / ^{240}\text{Pu} / ^{241}\text{Pu} / ^{242}\text{Pu}$ = 56 : 26 : 14 : 4
Pu enrichment	15.5 % in inner core 19.7 % in outer core

Table 2 Sensitivity of number density at EOC in various regions to cross sections

Number density	cross section	Sensitivity					
		Inner Core (1)	Outer Core (3)	Radial Blanket (5)	Blanket (6)	Axial Blanket (9)	Blanket (10)
^{239}Pu	^{238}U (n, γ)	0.2161	0.1349	0.3386	0.0927	0.3049	0.1806
	^{238}U -scattering	0.0119	0.0041	0.0339	-0.1239	0.0039	-0.0731
	^{239}Pu (n, γ)	-0.0600	-0.0430	-0.0153	0.0032	-0.0315	-0.0186
	^{239}Pu (n, f)	-0.1795	-0.1203	-0.3254	-0.2728	-0.3022	-0.2701
	^{16}O -scattering	0.0117	0.0052	0.0188	-0.1286	-0.0107	-0.0845
^{241}Pu	^{238}U (n, γ)	0.0121	-0.0119	-0.5760	-1.0623	-0.5020	-0.7911
	^{239}Pu (n, γ)	0.0125	0.0039	0.3373	0.2514	0.2278	0.2181
	^{239}Pu (n, f)	0.0802	0.0825	-0.8166	-0.6376	-0.6272	-0.5691
	^{241}Pu (n, γ)	-0.0516	-0.0375	-0.0121	0.0004	-0.0058	-0.0068
	^{241}Pu (n, f)	-0.2234	-0.1689	-0.2478	-0.1849	-0.2429	-0.2066

07140022

Table 3 Component-wise Total Sensitivity of ^{239}Pu
Number Density in Inner Core

Cross Section	N.D.	Flux	Power	Total
^{238}U Capture	2.337 -1	-1.760 -2	0.0	2.161 -1
Fission	-5.523 -4	3.640 -4	-1.342 -3	-1.530 -3
^{239}Pu Capture	-5.704 -2	-2.927 -3	0.0	-5.997 -2
Fission	-1.663 -1	-7.138 -3	-6.079 -3	-1.795 -1
^{240}Pu Capture	0.0	-1.333 -3	0.0	-1.333 -3
Fission	0.0	-2.453 -4	-5.012 -4	-7.465 -4
^{241}Pu Capture	0.0	-4.812 -4	0.0	-4.812 -4
Fission	0.0	-2.434 -3	-1.645 -3	-4.079 -3
^{242}Pu Capture	0.0	-1.330 -4	0.0	-1.330 -4
Fission	0.0	-2.114 -5	-6.385 -5	-8.499 -5
FP Capture	0.0	-1.007 -3	0.0	-1.007 -3
^{235}U Capture	0.0	-7.684 -5	0.0	-7.684 -5
Fission	0.0	-1.948 -4	-2.010 -4	-3.958 -4

07140023

Table 4 Total Sensitivity coefficient of k_{eff} at BOC and EOC to various cross sections and their components

Cross section	Total Sensitivity					
	BOC	EOC				
		Direct term	N.D.	Flux	Power	Total
^{238}U (n,r)	-2.44 -01	-2.44 -01	8.77 -02	-8.71 -03	0.0	-1.64 -01
^{238}U (n,f)	7.72 -02	8.07 -02	-1.27 -03	2.34 -04	2.53 -03	8.21 -02
^{238}U -transport	2.65 -02	2.51 -02	0.0	-2.87 -04	0.0	2.48 -02
^{238}U -scattering	-3.48 -02	-3.94 -02	0.0	3.93 -03	0.0	-3.54 -02
^{239}Pu (n,r)	-5.47 -02	-5.38 -02	-1.73 -02	-1.23 -03	0.0	-7.23 -02
^{239}Pu (n,f)	4.44 -01	4.63 -01	-6.91 -02	-2.98 -03	1.15 -02	4.02 -01
^{240}Pu (n,r)	-2.36 -02	-2.32 -02	1.14 -02	-5.19 -04	0.0	-1.22 -02
^{241}Pu (n,f)	1.25 -01	1.30 -01	-2.36 -02	-1.03 -03	3.11 -03	1.08 -01
FP (n,r)	-1.43 -02	-2.74 -02	7.57 -03	-3.20 -04	0.0	-2.02 -02

07140024

Table 5 Group-dependent sensitivity coefficients of k_{eff}
at BOC and EOC to cross sections of several heavy nuclides

cross section	Group No.	Sensitivity Coefficient	
		BOC	EOC
$^{238}\text{U}(n,\gamma)$	1	-9.54 -03	-7.11 -03
	2	-4.73 -02	-3.30 -02
	3	-1.64 -01	-1.09 -01
	4	-2.40 -02	-1.50 -02
^{238}U -scattering	1	-4.08 -02	-4.14 -02
	2	1.55 -04	4.90 -04
	3	5.85 -03	5.49 -03
	4	-3.10 -05	-5.90 -07
$^{239}\text{Pu}(n,\gamma)$	1	-7.28 -04	-8.89 -04
	2	-7.56 -03	-9.65 -03
	3	-3.41 -02	-4.63 -02
	4	-1.23 -02	-1.55 -02
$^{239}\text{Pu}(n,f)$	1	6.55 -02	3.13 -02
	2	1.49 -01	1.35 -01
	3	1.96 -01	1.77 -01
	4	3.42 -02	3.13 -02
Pseudo FP Capture	1	-3.39 -04	-5.33 -04
	2	-2.16 -03	-3.22 -03
	3	-8.91 -03	-1.26 -02
	4	-2.84 -03	-3.78 -03

Table 6 Total sensitivity of burnup reactivity loss

Cross section :	Total sensitivity
^{238}U Capture	-3.12
Fission	-2.86 -1
Scattering	6.13 -2
^{239}Pu Capture	7.94 -1
Fission	1.33
Scattering	6.02 -3
^{240}Pu Capture	-4.51 -1
Fission	-6.33 -2
Scattering	2.08 -3
^{241}Pu Capture	1.83 -1
Fission	5.71 -1
Scattering	1.10 -3
^{212}Pu Capture	-2.66 -2
Fission	-1.79 -2
Scattering	3.64 -4
F.P. Capture	-2.96 -1
Scattering	3.51 -3
^{56}Fe Capture	3.70 -2
Scattering	6.79 -2

Table. 7 Energy, Component wise Sensitivity of Burnup reactivity Loss
to $^{238}\text{U}(n,r), ^{239}\text{Pu}(n,f)$ cross sections

Cross section	Energy group	Sensitivity				
		Direct	N.D.	Flux	Power	Total
$^{238}\text{U}(n,r)$	1	0.015	-0.106	0.0002	0.0	-0.092
	2	0.060	-0.634	0.021	0.0	-0.552
	3	0.159	-2.614	0.335	0.0	-2.119
	4	0.005	-0.364	0.008	0.0	-0.352
	Sum	0.240	-3.718	0.363	---	-3.115
$^{239}\text{Pu}(n,f)$	1	-0.150	0.416	-0.0002	-0.069	0.196
	2	-0.399	0.994	0.021	-0.164	0.452
	3	-0.572	1.258	0.115	-0.208	0.592
	4	-0.091	0.230	-0.011	-0.040	0.089
	Sum	-1.238	2.896	0.125	-0.482	1.329

07140027

Table 8 Comparison of sensitivities from direct subtraction calculation and generalized perturbation calculation

- * sensitivity from direct subtraction
- ** sensitivity from generalized perturbation theory
- *** ratio (**/*)

neutronic properties		cross section change			
		^{238}U (n,r)	^{239}Pu (n,f)	FP (n,r)	
k_{eff} at BOC	*	-0.235	0.436	-1.42 -02	
	**	-0.244	0.444	-1.42 -02	
	***	1.04	1.02	1.00	
k_{eff} at EOC		-0.148	0.397	-2.76 -02	
		-0.157	0.408	-2.02 -02	
		1.00	1.03	0.73	
reactivity loss		-3.52	1.08	0.576	
		-3.42	1.08	0.262	
		0.97	1.00	0.45	
number density	^{239}Pu at inner core (1)		0.210	-0.169	-1.06 -03
		*	0.216	-0.180	-1.01 -03
		***	1.03	1.06	0.95
	^{239}Pu at radial blanket (1)		0.359	-0.567	1.22 -02
		*	0.339	-0.599	7.30 -03
		***	0.94	1.04	0.60

07140028

Fig.1 CALCULATIONAL FLOW DIAGRAM FOR N^* , Γ , Γ^* AND P^*

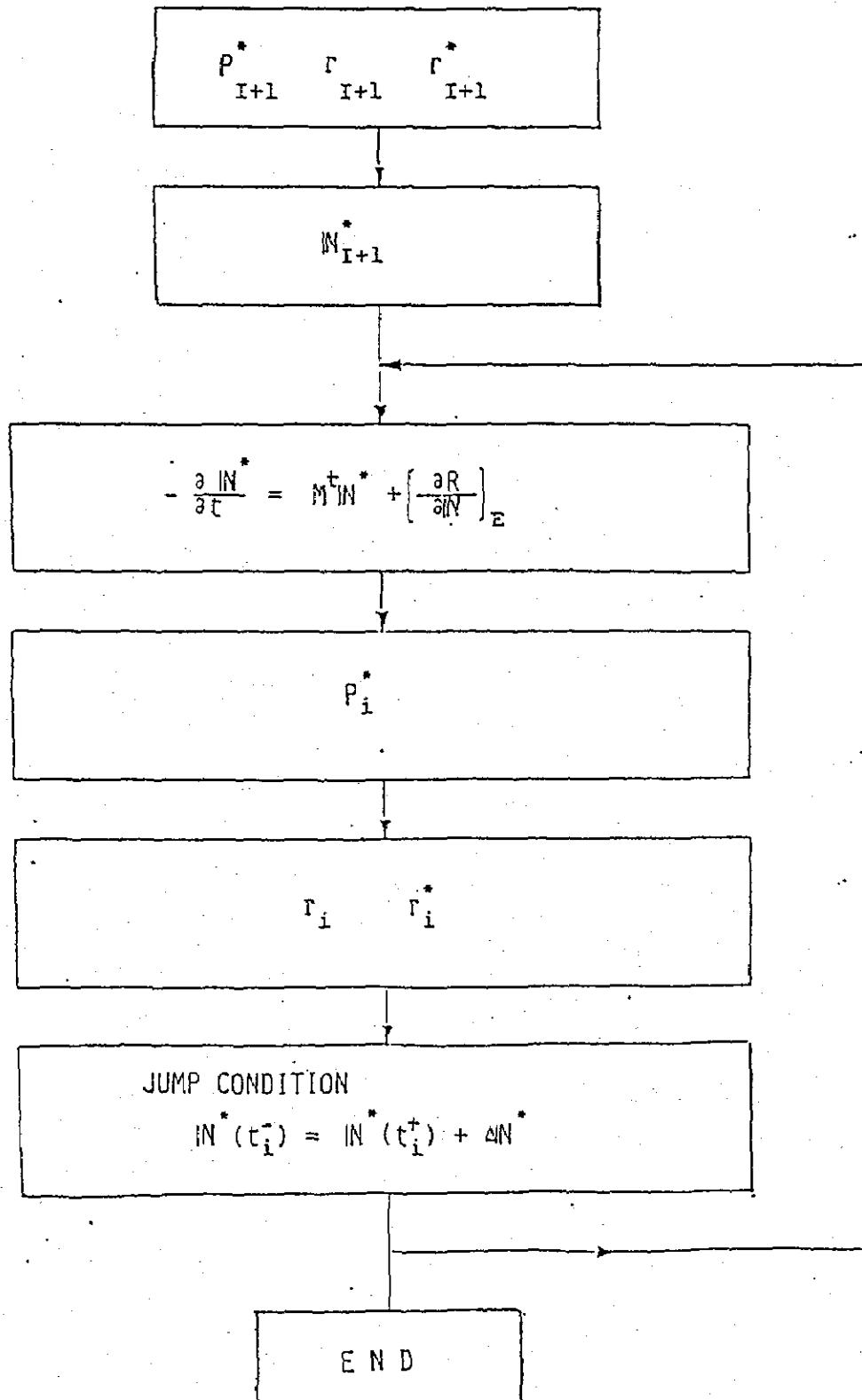


Fig. 2 RZ model of the target Reactor

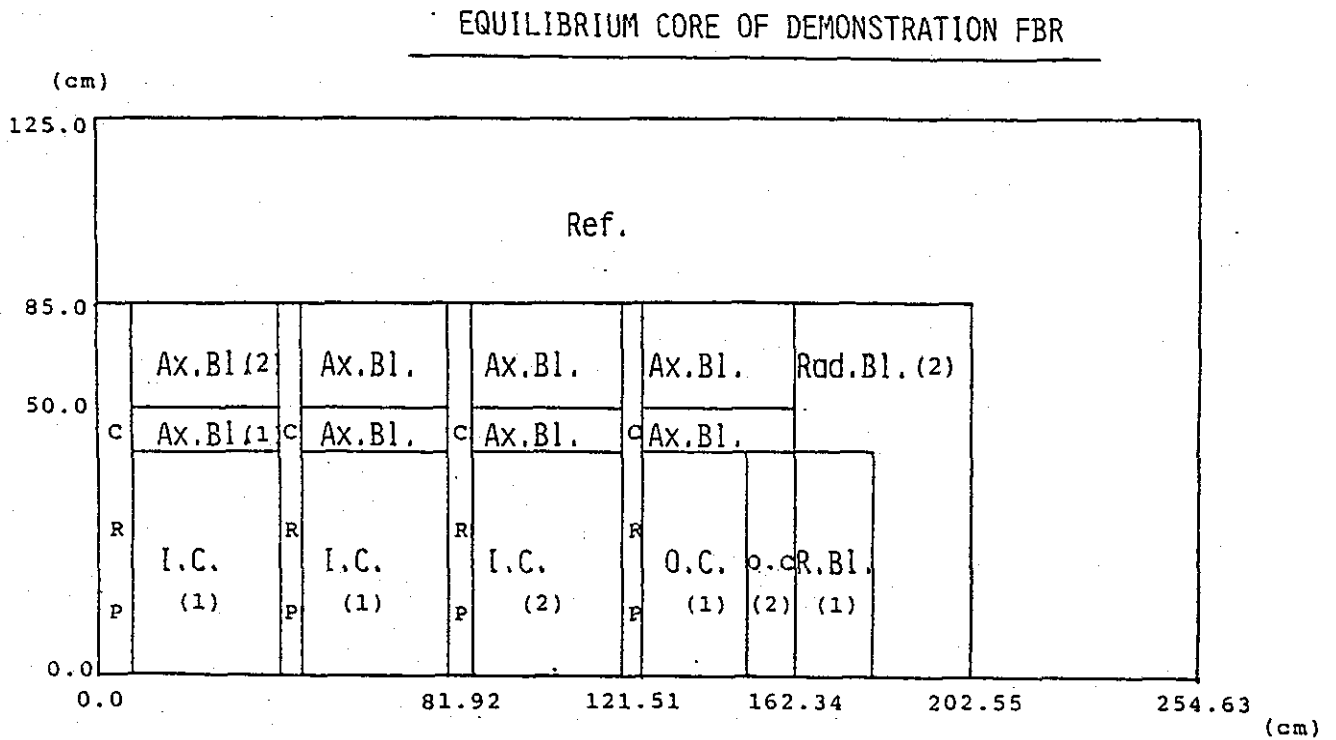
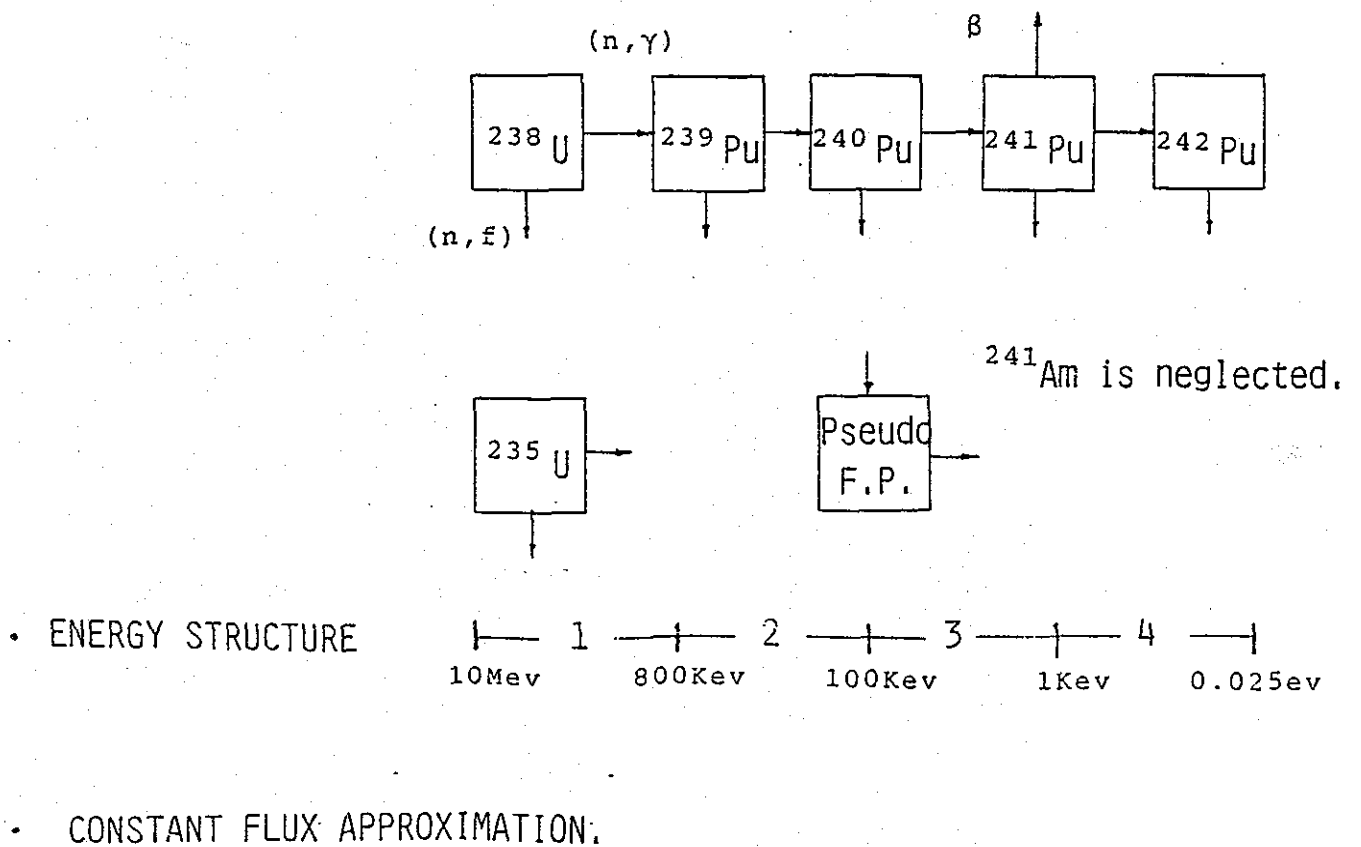


Fig. 3 Burn up chain



07140030